Steinberg, R. A., Levinson, B. B., & Tomkins, G. M. (1975) *Proc. Natl. Acad. Sci. U.S.A. 72*, 2007-2011.
Strauss, D. S., & Takemoto, C. D. (1987) *J. Biol. Chem. 262*, 1955-1960.
Thomas, P. S. (1980) *Proc. Natl. Acad. Sci. U.S.A. 77*, 5201-5205.
Yamashita, S., & Melmed, S. (1986) *J. Clin. Invest. 78*, 1008-1014.

Kinetic and Ultrastructural Studies of Interactions of Target-Sensitive Immunoliposomes with Herpes Simplex Virus†

Rodney J. Y. Ho,‡,§ H. P. Ting-Beall,‖ Barry T. Rouse,⊥ and Leaf Huang*,‡

Departments of Biochemistry and Microbiology, University of Tennessee, Knoxville, Tennessee 37996-0840, and Department of Anatomy, Duke University Medical Center, Durham, North Carolina 27710

Received May 20, 1987; Revised Manuscript Received September 17, 1987

ABSTRACT: The bilayer phase of dioleoylphosphatidylethanolamine (PE) can be stabilized with palmitoyl-IgG monoclonal antibody to the glycoprotein gD of the herpes simplex virus (HSV). Interactions of PE immunoliposomes with the target virions were characterized by analyzing the kinetics of lipid mixing, by liposomal content release, and by ultrastructural studies. As revealed by a resonance energy transfer assay, lipid mixing between PE immunoliposomes and virions was very rapid, with a second-order rate constant (k_{app}) of 0.173 $(min)^{-1}$ $(\mu g/mL\ virus)^{-1}$. In comparison, content release from PE immunoliposomes was much slower and exhibited multiple-phase, mixed-order kinetics, indicating that liposome destabilization involved fusion of liposomes with HSV. The extent and the apparent rate of liposome destabilization were strongly dependent on liposome concentration. This was evident by the fact that only one to two liposomes were destabilized by each virus particle at low liposome concentration (0.1 μM). For higher liposome concentrations (1-10 μM), this value was 35-104. This finding implies that collision among the virus-bound liposomes is essential for the eventual collapse of PE immunoliposomes to form the hexagonal (H_{II}) equilibrium phase which was observed using freeze-fracture electron microscopy. Studies employing soluble gD, immobilized on latex beads, indicated that a multivalent antigen source is essential for PE immunoliposome destabilization. Immediately after liposome-virus binding, fusion of liposome with the viral membrane then follows. Upon growth of the fusion complexes, which increase to 35-104 liposomes for each virus, an eventual collapse of the structure results, driving PE to its equilibrium structure of H_{II} phase.

We have recently reported preparation of novel, antibody-coated phosphatidylethanolamine (PE)[1] liposomes that can be readily destabilized by binding to target membranes expressing the antigen [target-sensitive immunoliposome (Ho et al., 1986a,b)]. Target-sensitive (TS) immunoliposomes were constructed by employing palmitoyl-IgG (pIgG) antibody against glycoprotein D (gD) of herpes simplex virus (HSV) to stabilize a PE bilayer (Ho et al., 1986a). By itself, PE assumes a nonbilayer, hexagonal (H_{II}) structure under physiological conditions [see Cullis and DeKruijff (1979), Siegel (1987), Isrealachvili et al. (1980), and Verkleij (1984) for reviews]. Using both intact virions and viral antigen expressing cells, we have shown that a specific interaction exists between TS immunoliposomes and immobilized, multivalent antigen gD which results in the destabilization of the liposomes. This was readily detected by the release of liposome-entrapped calcein and further demonstrated by using antiviral drugs (Ho et al., 1986a,b, 1987a,b).

Since all of the reported measurements were done at equilibrium or near the end point of the destabilization process (i.e., 30 min after liposome-virus mixing), the nature of the intermediate steps remains to be elucidated. Because the understanding of such molecular events is crucial to optimize TS immunoliposome-mediated antiviral drug delivery and to optimize the TS immunoliposome-based immune detection assay, we have further investigated the interactions of TS immunoliposomes with target HSV virions. In this report, we elucidate the mechanism of TS immunoliposome and HSV-gD interactions on the basis of kinetic studies of lipid mixing, liposomal content release, and ultrastructural studies of intermediates. The results showed that binding of TS immunoliposomes to target HSV is characterized by fast lipid mixing, fusion between liposome and virus, and a subsequent slower, multiple-phase content release, eventually leading to

† Supported by a contract from LipoGen, Inc., and by National Institutes of Health Grants CA24553, GM27804, and EY05093. L.H. was supported by a Research Career Development Award from NIH (CA00718), and R.J.Y.H. was a recipient of a Science Alliance Fellowship.

* Address correspondence to this author.
‡ Department of Biochemistry, University of Tennessee.
§ Present address: Division of Infectious Diseases, Stanford University School of Medicine, Stanford, CA 94305.
‖ Department of Anatomy, Duke University Medical Center.
⊥ Department of Microbiology, University of Tennessee.

[1] Abbreviations: PE, phosphatidylethanolamine; TS, target sensitive; pIgG, palmitoyl-IgG; gD, glycoprotein D; HSV, herpes simplex virus; DOPE, dioleoyl-PE; TPE, transphosphatidylated PE (from egg PC); PC, phosphatidylcholine; NBD-PE, *N*-(7-nitro-2,1,3-benzoxadiazol-4-yl)-PE; Rh-PE, *N*-(lissamine rhodamine B sulfonyl)-PE; EDCI, 1-ethyl-3-[3-(dimethylamino)propyl]carbodiimide hydrochloride; DOC, deoxycholate; PBS, phosphate-buffered saline; EGTA, ethylene glycol bis(β-aminoethyl ether)-*N*,*N*,*N*′,*N*′-tetraacetic acid; BSA, bovine serum albumin.

0006-2960/88/0427-0500$01.50/0

the conversion of the PE bilayer to the hexagonal (H_{II}) equilibrium phase.

Materials and Methods

Materials. DOPE, TPE, PC, *N*-(7-nitro-2,1,3-benzoxadiazol-4-yl)-PE (NBD-PE), and *N*-(lissamine rhodamine B sulfonyl)-PE (Rh-PE) were purchased from Avanti Polar Lipids (Birmingham, AL). Carboxylated latex beads of 0.99 μm (8828) were purchased from Polysciences, Inc. (Worrington, PA), 1-ethyl-3-[3-(dimethylamino)propyl]carbodiimide hydrochloride (EDCI) was from Chemical Dynamic Co. (South Plainfield, NJ), and all other reagents were analytical grade. Monoclonal antibody (D4.2) (originally isolated by Dr. Melvin Trousdale) to the glycoprotein D (gD) of herpes simplex virions (HSV) was purified and acylated with palmitic acid as described (Ho et al., 1986a).

Liposome Preparation. A self-quenching fluorescence marker, calcein, was entrapped in target-sensitive immunoliposomes composed of DOPE and palmitoyl-IgG (4000:1 mol/mol). Liposomes were prepared by sonication according to Ho et al. (1986a). Further details and modifications can be found in Ho et al. (1987a). Liposomes used in the lipid mixing experiment were prepared by the addition of 1 mol % each of Rh-PE and NBD-PE without calcein. These liposomes were passed through a Bio-gel A-0.5M column to remove the trace amount of deoxycholate (DOC) in the pIgG buffer (Ho et al., 1986a).

For ultrastructural studies, the sonicated immunoliposomes composed of DOPE, TPE, or PC without calcein were extruded through a 0.1-μm polycarbonate membrane, and residual DOC in the mixture was removed by dialysis against several changes of PBS containing 1 mM EGTA and 0.02% NaN_3.

Virus Preparation. The HF strain of HSV-1 was propagated in Hep-2 cells. After three cycles of freeze–thawing the infected monolayer, HSV was isolated from cell debris by an initial centrifugation at 10^3g for 10 min. The virus in the supernatant was pelleted by ultracentrifugation at 10^5g for 1.5 h. Resulting crude HSV virus was resuspended in a small volume of PBS, and enveloped virus was further purified with linear 20–50% potassium tartrate gradient centrifugation at (8×10^4g for 4 h according to Lopez and O'Rielly (1977). The resulting gradients were fractionated from the bottom of the tubes with a peristaltic pump, and fractions containing enveloped virus were diluted 50 times with PBS, and the virus was pelleted by centrifugation at 10^5g for 1.5 h. The virus pellet was resuspended in PBS, and protein concentration was determined to be 140 μg/mL (Lowry et al., 1951). Purified virus, which contains mainly enveloped HSV, was infectious and was stored in PBS at −70 °C.

Preparation of Latex Beads Conjugated with Truncated HSV Glycoprotein D. Affinity-purified, genetically engineered HSV–gD (Nar) (a gift from Dr. Berman and Dr. Lasky, Genetech Inc.; a 312 amino acid, soluble fragment of gD lacking the transmembrane segment referred to as tgD) was conjugated to carboxylated latex according to Kung et al. (1985), with modifications (Ho et al., 1987a). The final suspension contained 0.5% of tgD–beads, which is equivalent to 16 μg/mL tgD immobilized on latex. The resulting tgD–beads were shown previously to bind specifically to anti-gD IgG with a dissociation constant K_d of 1.5×10^{-8} M. This is similar to the K_d of the same IgG binding to the membrane-bound HSV gD [$K_d = 0.5 \times 10^{-8}$ M (Ho et al., 1986a)].

Kinetics of Lipid Mixing between TS Immunoliposomes and HSV. TS immunoliposomes containing 1 mol % each of NBD-PE and Rh-PE were used in these experiments. The resonance energy transfer efficiency between the donor fluorophore NBD-PE and the acceptor fluorophore Rh-PE incorporated in the TS immunoliposome is dependent on the surface density of the probe in the membrane. Upon fusion of these liposomes with HSV, the surface density of the fluorophores decreases, giving rise to an increase in the fluorescence intensity of the donor lipid NBD-PE (Struck et al., 1981; Hoekstra, 1982). Varying amounts of HSV were added to the liposome suspension of 1 μM (final concentration of lipid) in PBS containing 1 mM EGTA, and the increase in NBD fluorescence was continuously monitored at $\lambda_{ex} = 465$ nm and $\lambda_{em} = 530$ nm with a Perkin-Elmer LS5 spectrofluorometer. Total volume of the reaction mixture was 2 mL. The fraction of liposomes remaining unfused with viral membrane was determined by using the equation:

$$\text{fraction of unfused liposomes} = 1 - F/F_t$$

where F is the additional fluorescence induced by the presence of virus and F_t is the background-corrected total fluorescence after prolonged sonication to mechanically induce lipid mixing between virus and liposomes. The data were analyzed graphically by plotting ln $(1 - F/F_t)$ vs time to determine the first-order, apparent rate constant (k_{app}).

Kinetics of Virus-Induced Liposome Destabilization. To a liposome suspension containing 1 mM EGTA in PBS, at the indicated lipid concentration, an appropriate volume of virus was added, and the increase in calcein fluorescence due to release of calcein from destabilized liposomes was detected continuously with a Perkin-Elmer LS5 spectrophotometer at $\lambda_{ex} = 490$ nm and $\lambda_{em} = 520$ nm. Fluorescence values were presented as the percent of total calcein fluorescence. The total volume of the reaction mixture was kept constant at 2 mL. Using either tgD or anti-gD IgG in inhibition experiments, inhibitors were added to either the liposome suspension (tgD) or the HSV suspension (anti-gD IgG) 2 min prior to the mixing of liposomes with virus. All the experiments were done at 22 °C.

Liposome destabilization based on calcein release data was analyzed with the following assumptions. First, the change in calcein fluorescence over time is due to the destabilization of calcein-entrapped liposomes. The fraction of the total fluorescence is directly proportional to the concentration of destabilized liposomes in the suspension. Finally, virus-induced destabilization of liposomes yields a total release of the calcein entrapped in each liposome. Using these assumptions, we can estimate the fraction of stable liposomes remaining at a given time using the formula:

$$\text{fraction of stable liposomes} = 1 - F/F_t$$

where F is the fluorescence value due to virus addition at the indicated time and F_t is the total fluorescence increase upon total liposome lysis by the addition of 0.15% DOC in the absence of virus. The data were analyzed by plotting ln $(1 - F/F_t)$ vs time for first-order kinetic analysis and $(1 - F/F_t)^{-1}$ vs time for second-order kinetic analysis with respect to liposome concentration.

Kinetics of Interactions of TS Immunoliposomes with tgD–Beads. To calcein-entrapped liposomes 1 μM in PBS (containing 1 mM EGTA), varying amounts of tgD–beads were added, and destabilization of the TS immunoliposomes was monitored continuously with the LS5 spectrofluorometer as described above. The final volume was 2 mL. The fraction of stable liposomes remaining was also determined as above, the resulting data were plotted as ln $(1 - F/F_t)$ vs time, and the apparent first-order rate constants with respect to liposome concentration were determined. The replot of these rate

constants with the virus concentration gave an apparent overall second-order rate constant.

Electron Microscopy. Liposomes (20 μM) and virus (24 μg/mL) were mixed to initiate the reaction. At indicated times, 5 μL of the mixture was diluted to 50 μL with PBS and was immediately loaded onto a carbon-coated copper grid. With the exception of Figure 6B, all of the samples were negatively stained with 0.5% (w/v) potassium phosphotungstate. The liposome sample from the electron micrograph presented in Figure 6B was stained with 0.5% uranyl acetate.

Much higher final concentrations of virus (1 mg/mL) and liposomes (5 mM) were used in freeze–fracture studies. An aliquot (~0.1 μL) of liposome-virus mixture was loaded between two copper strips and was rapidly frozen in excess of 10^4 °C/s by plunging the resulting sample into liquid propane at −190 °C (Costello, 1980; Costello et al., 1982). Frozen samples were mounted in a double-replica device adapted for use in a Balzer 360 M freeze–fracture apparatus (Balzers Co., Nashua, NH) and fractured at −150 °C with a vacuum of 10^{-7} T. The fractured samples were immediately replicated with Pt/C at a 45° angle followed by C at a 90° angle. Procedures for replica processing have been published elsewhere (Costello et al., 1982; Ting-Beall et al., 1984). The resulting replicas were cleaned with Clorox and picked up on 400-mesh uncoated grids.

The replicas as well as the negatively stained samples were examined with a Phillip 301 electron microscope at 80 kV and 50-μm objective aperture.

RESULTS

Kinetics of Lipid Mixing between TS Immunoliposomes with HSV. In order to analyze membrane fusion between TS immunoliposomes and the envelope membrane of HSV, we employed a resonance energy transfer assay (Struck et al., 1981; Hoekstra, 1982). One percent each of NBD-PE and Rh-PE was incorporated into the bilayer of TS immunoliposomes, and the increase of NBD fluorescence was followed. The efficiency of resonance energy transfer between NBD-PE and Rh-PE decreases with the sixth power of the mean distance between the donor (liposomes) and acceptor (virus) (Förster, 1949) when the probes were diluted by lipid mixing. As can be seen in Figure 1A, the increase of NBD fluorescence was dependent on the concentration of virus added and was completed within a few minutes. No further increase of NBD fluorescence was observed even after a prolonged period of sonciation to mechanically induce complete lipid mixing. Under our experimental conditions, viral lipids appeared to be limiting. This is further evidenced by graphical analysis of ln $(1 - F/F_t)$ vs time (Figure 1B) which indicates an apparent first-order reaction. The overall k_{app}, the second-order rate constant of lipid mixing, was determined from the slope of the straight line in the Figure 1B insert to be 0.173 $(\mu g/mL)^{-1}$ min^{-1}. A similar rate of increase in (90°) light scattering (an indication of liposome–virus binding) further indicated that TS immunoliposome binding to virus was very rapid and was followed immediately by a complete mixing of lipid (data not shown). The similarity in kinetics between binding and lipid mixing did not allow us to separate the two events under our experimental conditions. This rapid lipid mixing between TS immunoliposomes and target HSV, that occurred immediately following the light-scattering increase, indicated the rapid fusion (either with or without mixing of aqueous contents) between liposomes and virus.

Kinetics of HSV-Induced TS Immunoliposome Destabilization. We have investigated the kinetics of HSV-induced destabilization of TS immunoliposomes by following the increase of calcein fluorescence upon the addition of HSV to the reaction mixture. When a 50 mM sample of a self-quenching dye, calcein, was stably entrapped inside these TS immunoliposomes, about 65–70% of the fluorescence was self-quenched. Upon release of calcein as the liposomes were destabilized, the increase of calcein fluorescence due to dilution can be used as a measure of membrane destabilization (Connor et al., 1984; Allen & Cleland, 1980). As can be seen in Figure 2A–C, the rate of calcein fluorescence increase was dependent on both liposome and HSV concentrations. In order to compare liposome destabilization rates, the percent total calcein fluorescence values in Figure 2A–C were converted to the equivalent amount (i.e., moles) of calcein released. When such conversions were used, the 1 and 10 μM concentrations of TS immunoliposomes gave the maximum rate as well as the amount of calcein released for the same amount of HSV added. Decreasing the liposome concentration to 0.1 μM gave a much lower fraction of the total fluorescence value at the end point. Furthermore, a nonexponential calcein fluorescence increase was also noted with the 1 μM liposome concentration. This concentration of liposomes gave multiple kinetic phases which took place over the time span of 15 min. This phenomenon was reproducible and was eliminated by either increasing or decreasing the liposome concentration (Figure 2A compared to Figure 2B,C). Further analysis showed that HSV-induced TS immunoliposome destabilization can be inhibited specifically either by preincubation of excess free anti-gD IgG (the same antibody incorporated in TS immunoliposomes) (Figure 2D) or by the addition of tgD to the liposomes (data not shown). However, the addition of excess anti-gD IgG after the completion of the first phase (see the arrow in Figure 2D) could not inhibit the subsequent increase of calcein fluorescence (Figure 2D). These findings indicate that the second phase of calcein release was not dependent on exposed antigenic sites accessible to antibody binding at that instant (Figure 2A,D).

Additionally, we have noted that as the concentration of HSV was increased, the time required to reach the end point

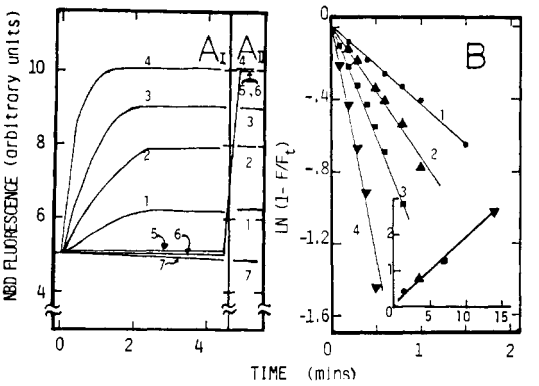

FIGURE 1: Kinetics of lipid mixing between TS immunoliposomes and herpes simplex virions. To 1 μM TS immunoliposomes containing 1% NBD-PE and 1% Rh-PE, varying concentrations of HSV were added, and the increase of NBD fluorescence due to lipid mixing between liposomes and virus was recorded (A_I). Lines 1, 2, and 3 represent 1.4, 3.5, and 7.0 μg/mL HSV, respectively; lines 4, 5, and 6 represent 14 μg/mL HSV; control experiment with no virus was represented by line 7. Inhibition by excess (70 μg/mL) tgD (line 5) and excess (70 μg/mL) anti-gD IgG (line 6) was also shown in panel A. NBD fluorescence after sonication to induce total lipid mixing was shown in A_{II}. The data from panel A were further analyzed by a first-order kinetic plot in panel B, and the same numbers as panel A were used to represent the virus concentration. In the insert of panel B, the apparent first-order rate constants (determined from slopes of the lines in panel B) were replotted against virus concentration in deducing the overall apparent second-order rate constant.

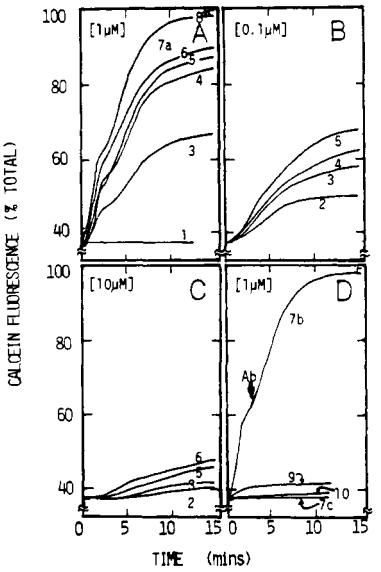

FIGURE 2: HSV-induced TS immunoliposome destabilization. To TS immunoliposome suspensions of 0.1 μM (B), 1 μM (A and D), and 10 μM (C) lipids, various amounts of HSV were added, and the increase of calcein fluorescence due to liposome destabilization was monitored. Final virus concentrations were 0 (line 1), 0.35 (line 2), 0.7 (line 3), 1.05 (line 4), 1.4 (line 5), 2.1 (line 6), and 2.5 (lines 7a–c, 9, and 10) μg/mL, respectively. Line 8 represents the total liposome-entrapped calcein fluorescence which was obtained by the addition of DOC. In panel D, the arrow indicates the addition of excess (70 μg/mL) anti-gD IgG to 2.5 μg/mL of an HSV-containing liposome–virus mixture (line 7b). In line 7C, 70 μg/mL anti-gD–IgG was preincubated with HSV before the addition of TS immunoliposomes. Control experiments were done with immunoliposomes composed of TPE (line 9) and PC (line 10).

of the first phase (for a 1 μM liposome suspension) was decreased although this time delay was not directly proportional to the virus concentration (Figure 2A).

The requirement for DOPE in the liposome bilayer was also studied. As shown in Figure 2D, substitution of DOPE with DOPC in the TS immunoliposome bilayer eliminated the ability of virus to induce liposome destabilization as indicated by the elimination of the virus-induced increase of calcein fluorescence. Replacement of DOPE with TPE, however, decreased the ability of virus to induce liposome destabilization, resulting in a lower amount of total calcein fluorescence observed under the same set of conditions (Figure 2D). These data indicate that under our experimental conditions, DOPE is the most efficient type of lipid for constructing TS immunoliposomes.

The calcein release data from Figure 2 were analyzed graphically by using first-order (Figure 3A–C) and second-order (Figure 3D–F) plots (Benson, 1960). For the 1 μM concentration of liposomes, at least three distinct phases could be discerned. From 0 to 2.4 min, destabilization of liposomes appeared to follow second-order kinetics with a subsequent delayed step that was prominent between 2.4 and 3 min for lower concentrations of virus (Figure 3E, lines 2, 4, and 5). This delayed step was eliminated by increasing the concentration of virus (lines 6 and 7a of Figure 3E). Between 4 and 6 min, the release of calcein appeared to follow a first-order process at virus concentrations between 1.05 and 2.1 μg/mL (see lines 4–6 of Figure 3B). Either at higher or at lower concentrations of liposomes, liposome destabilization appeared to follow at least two distinct second-order processes (Figure 3A,C,D,F), indicating that the overall reaction was a composite of several processes.

Therefore, the HSV-induced destabilization of TS immunoliposomes, detected by the increase of calcein fluorescence,

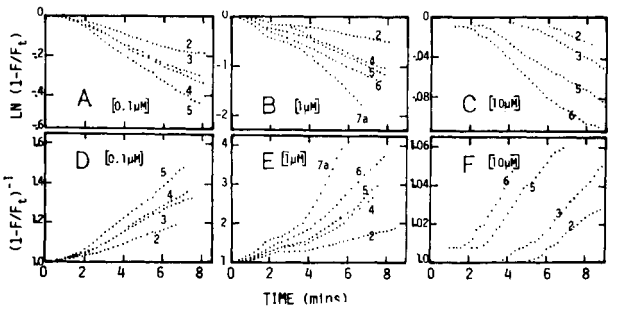

FIGURE 3: Kinetic analyses of HSV-induced TS immunoliposome destabilization. Calcein release data from Figure 2 were further analyzed by employing first-order kinetic plots (A–C) and second-order kinetic plots (D–F). Panels A and D represent 0.1 μM, B and E represent 1 μM, and C and F represent 10 μM liposomal lipids, respectively. The same numerical representations for concentration as those of Figure 2 were used.

Table I: Estimation of the Number of TS Immunoliposomes Destabilized by Each Herpes Simplex Virion

	liposome concentration[b]		
[HSV][a] (μg/mL)	0.1 μM	1.0 μM	10 μM
0.35	5.3		103.3
0.70	4.3	60.5	90.5
1.05	3.3	63.8	84.0
1.40	3.3	52.3	73.0
2.1		35.8	
2.5		35.0	

[a] Initial concentration of virus added. [b] Initial concentration of liposomal lipid in the reaction mixture.

exhibited a strong dependence on liposome concentration which followed mixed-order kinetics with respect to liposome concentration. This mixed-order kinetics was also dependent on the virus concentration but could not be accounted for solely by the concentration of virus present.

Number of TS Immunoliposomes Destabilized by Each Virus. Liposome destabilization data from Figure 2 were analyzed further in an attempt to estimate the number of liposomes that could be destabilized by each virus particle. Since the size of this herpes virion is 1500–2000 Å in diameter (Hsuing, 1982; this report), and assuming the virus is spherical with an average diameter of 1800 Å, the surface area can be estimated to be 1.02×10^{-9} cm^2. The average cross-sectional area of the liposome is 1.96×10^{-11} cm^2, using the estimated liposome diameter of 500 Å (Ho et al., 1986a; this report). On the basis of these numbers, we estimated that each virus particle can accommodate a maximum of 52 liposomes (one layer thick).

In order to measure experimentally the number of liposomes destabilized by each virus particle, we made an assumption that there were 2×10^4 phospholipid molecules per 500-Å TS immunoliposome (Enoch & Strittmatter, 1979) or 6×10^{10} liposomes in 2 mL of the reaction mixture of 1 μM liposome suspension. An additional assumption was made according to Gentry and Randall (1973) in estimating HSV protein content to be 3×10^{-15} g/virion or 3.33×10^8 virions/μg of viral protein. On the basis of these assumptions, the experimental number of liposomes destabilized per virion was calculated from the data presented in Figure 2A–C (at the 14-min time point) and in Table I. The number of liposomes destabilized by each virus was much less at lower liposome concentrations and began to reach a maximum at about the 1 μM concentration of liposomal lipid. While the number of liposomes destabilized by each virion was shown to be about 10-fold lower for the 0.1 μM liposome concentration for the same amount of virus added, liposomes did not appear to be

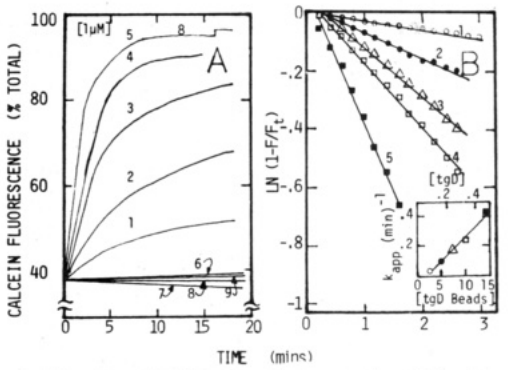

FIGURE 4: Kinetics of TS immunoliposome destabilization by immobilized antigen tgD–beads. (Panel A) In a quartz cuvette containing 1 μM TS immunoliposomes (encapsulated with calcein), various amounts of tgD–beads were added to a final tgD–bead concentration of 0.0025% (line 1), 0.005% (line 2), 0.0075% (line 3), 0.01% (line 4), and 0.015% (lines 5–7). This is equivalent to tgD protein concentrations of 0.08, 0.16, 0.24, 0.32, and 0.48 μg/mL, respectively. For inhibition experiments, TS immunoliposomes were preincubated with 14 μg of tgD (line 6), or tgD–beads were preincubated with 70 μg of anti-gD IgG (line 7) before the initiation of reactions. Additional control experiemnts were done with BSA-immobilized beads (line 8) or PC immunoliposomes (line 9). (Panel B) The calcein release data from panel A were plotted on a first-order kinetic plot using the same numerical representation of tgD or tgD–bead concentration as that of panel A, and the insert shows the replot of the slopes that give apparent second-order rate constants.

limiting since only a fraction of the total liposome-entrapped calcein was released after 35 min (see Figure 3B and Table I). This result indicated that at least 14 liposomes per virus were necessary to induce full release of entrapped calcein and, hence, total collapse of the liposome–virus complex. Additionally, 35–103 liposomes per virus appeared to be the optimum ratio for liposome destabilization that exhibited the highest initial rates. Experimental estimation of the saturation number was in reasonably good agreement with the theoretical value of 52 liposomes per virion. Thus, we conclude that each virus can destabilize a maximum of 73–103 TS immunoliposomes 500 Å in size.

Kinetics of Interactions of TS Immunoliposomes with Immobilized Antigen. We next addressed the questions of multivalent antigen requirement for destabilization of TS immunoliposomes and if antigen immobilized on latex beads acted the same as did native antigen expressed on virions. The antigen conjugated to latex beads was a genetically cloned HSV-gD without a transmembrane segment (a soluble form of gD, tgD) (Berman et al., 1984). When tgD immobilized on latex beads (tgD–beads) was added to the liposome suspension at 1 μM, the extent (Figure 4A) and the rate (Figure 4B) of TS immunoliposome destabilization were shown to be dependent on the concentration of tgD–beads. Kinetic analyses showed that the rate of liposome destabilization followed apparent first-order kinetics with respect to liposome concentration as well as tgD–bead concentration and it gave an overall apparent second-order rate constant of $k_{app} = 31.62$ min^{-1} (% tgD–beads)$^{-1}$ or 0.988 min^{-1} (μg of tgD/mL)$^{-1}$ (Figure 4B). In addition, the tgD–bead-induced destabilization of TS immunoliposomes can be inhibited by preincubation of tgD with TS immunoliposomes while the soluble tgD alone could not bring about destabilization of TS immunoliposomes (Figure 4A). Similar inhibition was also observed with preincubation of tgD–beads with anti-gD IgG, indicating that the interaction was gD epitope specific. In order to rule out the possibility that a contact between latex and bilayer alone could promote liposome destabilization, immunoliposomes composed of PC were used as a control. As can be seen in Figure 4A, tgD–beads could not induce destabilization of such liposomes. Therefore, destabilization of TS immunoliposome by tgD required a multivalent antigen source, exhibited an apparent second-order reaction process, and was distinctively different from the mixed-order process observed with HSV virions.

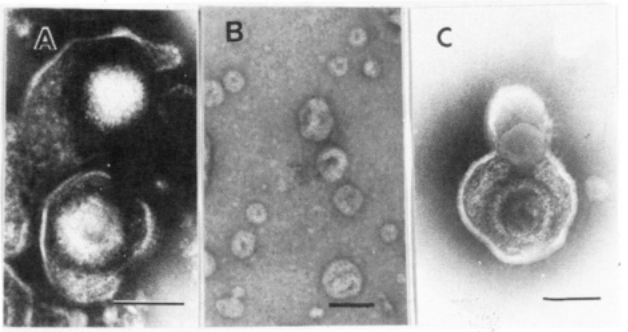

FIGURE 5: Negative-stain electron micrograph of HSV, TS immunoliposomes, and liposome–virus fusion intermediates. After mixing of herpes virions (A) and TS immunoliposomes (B) for 30 s, fusion intermediates such as the one shown in panel C were detected. The bars indicate 0.1 μm.

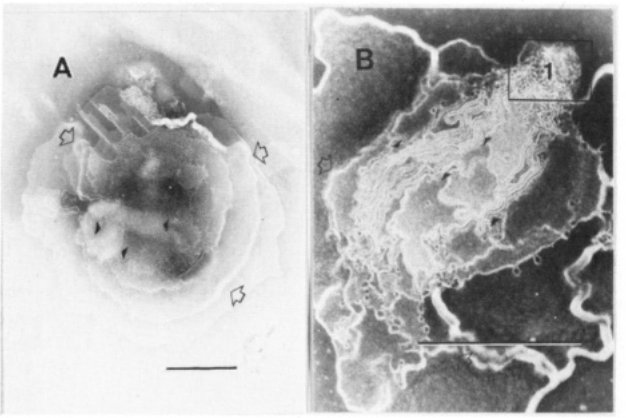

FIGURE 6: Negative-stain electron micrographs of TS immunoliposome–HSV fusion complexes. After 2 min of the reaction, TS immunoliposome–virus complexes (A and B) were detected. Arrows in panels A and B indicate the membrane stacking structures which might lead to the formation of the tubular structure of the hexagonal phase (arrowhead). Dissembly of nucleocapsid can be seen in area 1 of panel B. The bars indicate 0.5 μm.

Ultrastructural Studies of TS Immunoliposome–HSV Interactions. Due to the multiple steps involved in the HSV-induced release of calcein from the TS immunoliposomes (Figures 2 and 3), and due to the fact that this phenomenon was eliminated with tgD–bead-induced liposome destabilization, we reasoned that there may be several intermediate events involved in virus–liposome interactions. If this is the case, these intermediates might be observed by ultrastructural techniques. Hence, both negative-stain electron microscopy and freeze–fracture electron microscopy were employed to detect liposome–virus intermediates. As shown in Figure 5, upon mixing of TS immunoliposomes (Figure 5B) with HSV (Figure 5A), a fusion intermediate can be detected (Figure 5C). These fusion intermediates were short-lived ($t_{1/2} < 30$ s) and quickly grew to much larger multiple fusion complexes (Figure 6A,B). The viral nucleocapsids appeared to be disassembled in the fusion intermediates (Figure 5C), and total collapse of the nucleocapsid structure was seen in the larger fusion complexes (Figure 6A,B). When DOPE in TS immunoliposomes was replaced with either TPE or PC, only grossly aggregated liposome–virus complexes were seen (micrograph not shown).

When these samples were observed by freeze–fracture electron microscopy, we could not detect the intermediate

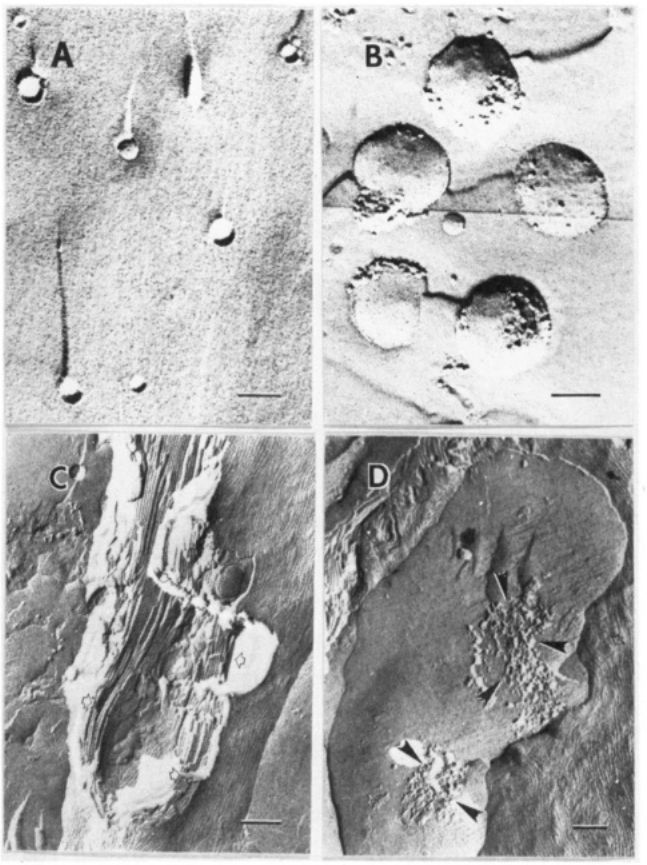

FIGURE 7: Freeze–fracture electron micrographs of TS immunoliposome–HSV interactions. Addition of herpes simplex virion (B) to immunoliposomes (A) resulted in the structures with apparent discontinuous tubular lipids shown in panels C and D. The arrows indicate the discontinuous tubular structure of the H_{II} phase, and the arrowheads indicate the viral protein particles that appear to be excluded from tubular structures of lipids. The bars indicate 0.1 μm.

structure before the TS immunoliposomes were converted to the H_{II} equilibrium phase (Figure 7C,D) probably due to a much higher concentration (about 500-fold) of liposomes and virus used. As shown in Figure 7, when TS immunoliposomes (Figure 7A) and HSV (Figure 7B) were mixed, a freeze–fracture electron micrograph showed that the final equilibrium phase consisted of extensive tubules characteristic of the hexagonal phase (Figure 7C,D) which apparently excluded viral nucleocapsid proteins (Figure 7D).

Taken together, negative-stain and freeze–fracture electron micrographs showed that HSV-induced destabilization of TS immunoliposomes involved multiple steps. These include initial virus–liposome binding, that becomes multiple fusion intermediates which appeared to dissemble the viral nucleocapsid, and, finally, rearrangement of the lipids to become the H_{II} equilibrium phase that excludes proteins. At present, we cannot quantitatively define the time frame and the extent of each event which corresponds to multiple kinetic steps observed in the calcein release experiments shown in Figure 2A.

Discussion

In our previous reports, we have established that target-sensitive (TS) immunoliposomes can be destabilized specifically by the target antigen gD which is multivalently expressed on either HSV virions or infected cells (Ho et al., 1986a,b). Additionally, we have shown that the lipid from TS immunoliposomes remains associated with the HSV even after the destabilization (Ho et al., 1987a). In this report, we have further characterized these interactions by studying the kinetics of lipid mixing, content release from the liposomes, and the requirement for multivalency of the antigen. We observed a much faster apparent rate (Figure 1) of lipid mixing compared to the rate of calcein release (Figures 2 and 3), indicating that binding and fusion alone were not the only events of the liposome destabilization resulting in calcein release. Instead, these events represent the initial steps that lead to the final collapse of the TS immunoliposomes in allowing PE to form the H_{II} equilibrium phase (Figures 5–7). In addition to the ultrastructural evidence for fusion intermediates, multiple phase calcein release kinetics further supported our hypothesis.

Since we do not yet have a reasonable estimate as to the fraction of calcein fluorescence contributed by binding, fusion, growth of fusion intermediates, and finally the bilayer collapse to form the H_{II} phase, estimation of the rate constant for each event using the mass action method is not possible at present. In addition, the use of higher concentrations of the virus was limited experimentally by the increase in the light scattering which interfered with fluorescence measurements. As a result, attempts to deduce kinetic constants for the release of entrapped markers (i.e., calcein) from TS immunoliposome–HSV interactions have met with little success. However, the total number of liposomes destabilized by each virion was shown to be dependent on liposome concentration. This is evidenced by the fact that only a small number (three to five) of liposomes were destabilized by each virion for 0.1 μM liposomes, under conditions where the liposome concentration was not limiting (Table I and Figure 2B). Since we could not measure lipid mixing due to the relatively low sensitivity of the resonance energy transfer assay at this particular concentration of liposomes, we could not rule out the possibility that nonleaky fusion intermediates did not contribute to an increase of calcein fluorescence. Nevertheless, the findings of at least a 10-fold higher number of liposomes destabilized per virion (in the range of 35–103, Table I) at higher liposome concentrations indicated that binding of a minimum of 35 liposomes is likely required to totally destabilize the virus–liposome fusion complexes. This hypothesis further implies that collision among the adjacent liposomes on the same virion may be essential for release of liposome-encapsulated contents. TS immunoliposome destabilization by liposome collision was further supported by the finding that the calcein fluorescence increase after 2 min was not inhibitable by the addition of excess antibody (see Figure 2D).

The requirement of liposome collision for the destabilization of PE liposomes was proposed previously (Ellens et al., 1984; Bentz et al., 1985; Hu et al., 1986). However, all these studies required about 20 μM liposomal lipid concentration to obtain reasonable kinetics. Inclusion of antibody in the PE liposomes in our case has allowed us to use lower concentrations of liposomes ($\leq$1 μM) to detect PE bilayer destabilization by the target HSV membrane. This is probably due to the specific binding of the liposomes to targets that can bring the membranes into close contact. In our system, membrane contact is probably required but not sufficient to cause TS immunoliposome destabilization.

Initial destabilization of TS immunoliposomes requires a multivalent binding between anti-gD IgG (on TS immunoliposomes) and gD (on virus or tgD–beads). This requirement is evidenced by the fact that a soluble antigen alone could not bring about the destabilization of TS immunoliposomes, whereas the same antigen, tgD, immobilized on latex (tgD–bead) was a potent destabilizer (Figure 4). Due to the complex kinetic data observed with herpes virions (Figures 2 and 3), we do not have a reasonable rate constant to compare the k_{app} of tgD–beads to that of HSV. The lipid mixing k_{app} of 0.173

min^{-1} (μg of HSV protein/mL)$^{-1}$ could not be used for comparison since only a small fraction of liposomes may actually be destabilized to release calcein, and furthermore, only a small fraction of viral protein is gD. Nonetheless, the studies of interactions between tgD–beads and TS immunoliposomes strongly indicated that multivalent and/or immobilized antigen, but not soluble antigen, is essential for the destabilization of TS immunoliposomes. These findings are consistent with our hypothesis, published elsewhere (Ho et al., 1986a,b), that lateral phase separation of the TS immunoliposome components is required for PE membrane destabilization. Taken together, our data indicate that initial destabilization by multivalent binding may promote liposome–virus fusion products that eventually collapse as the liposome–virus–fusion complexes grow to larger size.

Due to the experimental limitations at present, we cannot deduce absolute constants for each event that may be taking place following TS immunoliposome binding to their target HSV. However, we have observed some intermediates using ultrastructural methods which showed that specific binding of the TS immunoliposomes to target HSV is followed by formation of fusion intermediates which grow to become larger fusion complexes and eventually collapse and lead to formation of the H_{II} phase as the equilibrium structure (Figure 5–7). Whether the same events take place in TS immunoliposome binding to other membranes such as the HSV-infected cell membrane, however, remains to be elucidated.

In summary, we have shown that HSV-induced TS immunoliposome destabilization involves rapid lipid mixing and complex fusion between liposomes and virions that results in complex multiple kinetics of calcein release. These observations may be applicable in designing a site-specific liposome-mediated drug delivery system as well as constructing liposome-based assays for immune detection.

ACKNOWLEDGMENTS

We thank Dr. S. Martin for affinity purification of tgD, Dr. P. W. Berman and Dr. A. Lasky for providing tgD, Dr. J. Victor for permission to use the monoclonal D4.2, and Carolyn Drake for assistance in preparation of the manuscript.

Registry No. Dioleoyl-PE, 2462-63-7.

REFERENCES

Allen, T. M., & Cleland, L. G. (1980) *Biochim. Biophys. Acta 597*, 418–426.

Benson, S. W. (1960) in *The Foundation of Chemical Kinetics*, pp 3–25, McGraw-Hill, New York.

Bentz, J., Duzgunes, N., & Nir, S. (1985) *Biochemistry 24*, 1064–1072.

Berman, P. W., Dowbenko, D. J., Simonsen, C. C., & Lasky, L. A. (1984) in *Herpesvirus* (Rapp, F., Ed.) pp 637–649, Alan R. Liss, New York.

Connor, J., Yatvin, M. B., & Huang, L. (1984) *Proc. Natl. Acad. Sci. U.S.A. 81*, 1715–1718.

Costello, M. J. (1980) *Scanning Electron Microsc. 2*, 361–370.

Costello, M. J., Fetter, R., & Hochli, M. (1982) *J. Microsc. (Oxford) 125*, 125–136.

Cullis, P. R., & DeKruijff, B. (1979) *Biochim. Biophys. Acta 559*, 399–420.

Ellens, H., Bentz, J., & Szoka, F. C. (1984) *Biochemistry 23*, 1532–1538.

Enoch, H. G., & Strittmatter, P. (1979) *Proc. Natl. Acad. Sci. U.S.A. 76*, 145–149.

Förster, T. (1949) *Z. Naturforsch., A: Astrophys., Phys. Phys. Chem. 4A*, 321–327.

Gentry, G. A., & Randall, C. C. (1973) in *The Herpesviruses* (Kaplan, A. S., Ed.) pp 45–86, Academic Press, New York.

Ho, R. J. Y., Rouse, B. T., & Huang, L. (1986a) *Biochemistry 25*, 5500–5506.

Ho, R. J. Y., Rouse, B. T., & Huang, L. (1986b) *Biochem. Biophys. Res. Commun. 134*, 931–937.

Ho, R. J. Y., Rouse, B. T., & Huang, L. (1987a) *J. Biol. Chem. 262*, 13973–13978.

Ho, R. J. Y., Ting-Beall, H. P., Rouse, B. T., & Huang, L. (1987b) *Biophys. J. 51*, 115a.

Hoekstra, D. (1982) *Biochemistry 21*, 2833–2840.

Hsiung, G. D., Ed. (1982) in *Diagnostic Virology*, pp 77–86, Yale University Press, New Haven, CT.

Hu, L. R., Ho, R. J. Y., & Huang, L. (1986) *Biochem. Biophys. Res. Commun. 147*, 973–978.

Israelachvili, J. N., Marcelja, S., & Horn, R. G. (1980) *Q. Rev. Biophys. 13*, 121–200.

Kung, V. T., Maxim, P. E., Veltri, R. W., & Martin, F. J. (1985) *Biochim. Biophys. Acta 839*, 105–109.

Lopez, C., & O'Reilly, R. J. (1977) *J. Immunol. 118*, 895–901.

Lowry, O. H., Rosebrough, N. Y., Farr, A. L., & Randall, R. J. (1951) *J. Biol. Chem. 193*, 265–275.

Siegel, D. P. (1987) in *Cell Fusion* (Sowers, A. E., Ed.) Chapter 9, pp 181–207, Plenum Press, New York.

Struck, D. K., Hoekstra, D., & Pagano, R. E. (1981) *Biochemistry 20*, 4093–4099.

Ting-Beall, H. P., Holland, V. F., Freytag, J. W., Lewis, W. S., & Hastings, D. F. (1984) *Biochim. Biophys. Acta 776*, 190–196.

Verkleij, A. J., van Echteld, C. J. A., Gerritsen, W. J., Cullis, P. R., & DeKruijff, B. (1980) *Biochim. Biophys. Acta 600*, 620–624.